BREAST

Maximum slope using ultrafast breast DCE-MRI at 1.5 Tesla: a potential tool for predicting breast lesion aggressiveness

Margaux Pelissier[1] · Khalid Ambarki[2] · Julia Salleron[3] · Philippe Henrot[1]

Abstract

Objectives We evaluated the relationship between the maximum slope (MS) based on ultrafast breast DCE-MRI sequences, and the clinical parameters and routine prognostic factors of breast cancer.

Methods 210 lesions were retrospectively evaluated: 150 malignant (30 each of luminal A invasive carcinoma, luminal B invasive carcinoma, HER2 overexpression (HER2), triple negative (TN), invasive lobular carcinoma (ILC)), and 60 benign. For each lesion, the MS was obtained with an ultrafast sequence and semi-quantitative curves were classified into three types with a conventional DCE sequence. The correlation between MS and age, body mass index (BMI), menopause, and routine prognostic factors were analyzed.

Results A MS cut-off at 6.5%/s could discriminate benign from malignant lesions, with sensitivity and specificity of 84% and 90%, respectively, whereas analysis of semi-quantitative curves showed sensitivity and specificity of 89.3% and 55%, respectively. In multivariate analysis, MS values decreased with BMI increasing ($p = 0.035$), postmenopausal status ($p < 0.001$), and positive ER status ($p < 0.001$) and increased with tumor size ($p < 0.001$). The MS was significantly lower for the pooled luminal A + ILC group than for the pooled luminal B + HER2 + TN group featuring tumors with poorer prognoses ($p < 0.001$). With a threshold of 11%/s, the sensitivity and specificity to identify invasive carcinoma subtypes with poorer prognoses were 71% and 68%, respectively.

Conclusion The MS allows better tumor characterization and identifies factors of poor prognosis for breast cancer.

Key Points
• *Maximum slope calculated from ultrafast breast DCE-MRI differentiates benign from malignant breast lesions better than semi-quantitative curves of conventional DCE-MRI.*
• *Maximum slope calculated from ultrafast breast DCE-MRI identifies breast cancers with poor prognoses.*
• *In the case of multiple lesions, the most aggressive may be identified and targeted by measuring the maximum slope.*

Keywords Breast neoplasms · Magnetic resonance imaging · Kinetics · Prognosis

Abbreviations

AUC	Area under the curve
BMI	Body mass index
CI	Confidence interval
ER	Estrogen receptor
HER2	HER2 overexpression
ILC	Invasive lobular carcinoma
IQR	Interquartile range
LNI	Lymph node invasion
LVI	Lymphovascular involvement
MS	Maximum slope
PR	Progesterone receptor
SBR	Scarff–Bloom–Richardson
TN	Triple negative
TWIST	Time-resolved angiography with interleaved stochastic trajectories
VIBE	Volumetric interpolated breath–hold examination

✉ Philippe Henrot
p.henrot@nancy.unicancer.fr

[1] Department of Radiology, Institut de Cancérologie de Lorraine, 6 avenue de Bourgogne, 54 519 Vandoeuvre-les-Nancy, France

[2] Siemens Healthcare GmbH, Siemens Healthcare SAS, Saint Denis, France

[3] Department of Biostatistics, Institut de Cancérologie de Lorraine, 6 avenue de Bourgogne, 54 519 Vandoeuvre-les-Nancy, France

Introduction

MRI is the most sensitive technique for breast cancer diagnosis. Its sensitivity is reported to be between 87 and 99%, and its specificity between 72 and 81% [1–3].

Morphological analysis of lesions prevails over analysis of enhancement kinetics for the determination of BI-RADS (breast imaging reporting and database system) categories [4–7]. Enhancement analysis is a complementary method to improve specificity, especially in the case of lesions that are classified as indeterminate or probably benign by morphological analysis.

The first studies that indicated early enhancement rate (in the first 2 min) to be related to cancer, reported limited specificity [8–11]. Kuhl et al reported in 1999 the utility of a semi-quantitative analysis using enhancement curves obtained from DCE sequences, with a total acquisition duration of 7 min. Considering type 2 and type 3 (plateau and wash-out time courses) as diagnostic criteria of cancer and type 1 (steady enhancement) suggestive of benign lesion, the specificity was 83% versus 37% for enhancement rate alone [12]. In this study, the limitations of semi-quantitative study were highlighted; 17% of benign lesions presented enhancement of type 2 and 3 curves, and 8.9% of cancers presented enhancement of type 1 [12].

The recent introduction of new ultrafast dynamic sequences of the entire breast volume enables analysis of the early enhancement (wash-in) [13–15].

The application of ultrafast sequences to breast imaging was first reported by Hermann in 2011 [16] and its application in lesion characterization was reported by Mann et al in 2014 [14].

The maximum slope (MS) of enhancement obtained during the first minute expressed in percentage of signal per second has been reported to be among the parameters that more accurately predict malignancy.

Mann reported a sensitivity of 90% and a specificity of 67% with a MS threshold of 6.4%/s, and a specificity of 85% for a sensitivity of 65% with a MS threshold of 13.3%/s [14].

The aim of the present study was to investigate the diagnostic performance of the MS based on an ultrafast DCE-MRI sequence in breast malignant and benign lesions from a population diagnosed with breast cancer. The correlations between the MS and clinical and prognostic factors were analyzed.

Materials and methods

Type of study

This single-center, retrospective observational study was conducted in a comprehensive cancer center.

Population

The institutional review board of our institution approved this observational study and consent was waived for all subjects.

We carried out retrospective recruitment from a population of 1963 patients who had undergone breast MRI in our institution in the context of breast cancer on a single MRI scanner using the same examination protocol, from July 2015 to December 2018. Inclusion criteria were histology of invasive ductal carcinoma not otherwise specified (IDC NOS) or invasive lobular carcinoma (ILC), and an acquisition protocol including ultrafast TWIST (time-resolved angiography with interleaved stochastic trajectories)-VIBE (volumetric interpolated breath–hold examination) (TWIST-VIBE) sequences and dynamic gradient-echo VIBE sequences. Benign lesions selected in the study were only masses, excluding non-mass enhancements. Benignity was defined as benign histology, or the absence of cancer at 2 years checked with any imaging modality in the absence of histological verification.

Collection of data

Individuals were included in order of creation of the medical files until we reached 150 cases of malignant lesions, comprising: 30 IDC NOS of luminal A subtype (luminal A), 30 IDC NOS of luminal B subtype (luminal B), 30 IDC NOS with HER2 (HER 2), 30 TN IDC NOS (TN), and 30 ILC. The benign lesions were selected from imaging reports, in order of creation of the files until 60 lesions were obtained. Fifty-five lesions were selected in concomitant contralateral breast cancer and 1 in homolateral (proved to correspond to an adenofibroma). Four benign lesions were selected in patient followed-up after treatment. Among these, 23 were histologically verified, revealing 13 fibroadenomas, 4 inflammatory cysts, 1 area of dystrophy and ductal ecstasy, 2 intramammary lymph nodes, 1 area of adenoma, and 2 without specific histology.

Clinical data and antecedents

Data collected from the medical record were age, BMI, menopausal status, family history of breast cancer (at least one first-degree relative), and genetic family risk of breast cancer. Moderate and high risk corresponded to a lifetime risk of breast cancer determined by oncogenetic investigation > 12% and > 20% respectively.

Lesion size and pathological data

For operated lesions, the lesion size was determined by anatomo-pathological analysis. For lesions treated with neo-adjuvant chemotherapy, the lesion size was determined by imaging work-up. Pathological data (after resection or biopsy)

included the immunophenotype: hormone receptor status (percentage of cells positive for ER and PR), HER2 status (positive or negative), ki67-index value, SBR grading, presence of lymphovascular involvement (LVI), and presence of lymph node invasion (LNI).

Tumors were classified by molecular and histological subtype. We retained the European positivity threshold of 10% of tumor cells for determining the status of hormone receptors: luminal A: ER $\geq$ 10%, PR $\geq$ 10%/ HER2 negative, Ki67 $\leq$ 15% IDC NOS; luminal B: ER $\geq$ 10%, PR $\geq$ 10%, or < 10%, HER2 negative, Ki67 > 15% IDC NOS; HER2: HER2 rated 3+ or 2+ amplified IDC NOS; TN: ER < 10%, PR < 10%, HER2 negative $\leq$ IDC NOS.

The MS was evaluated for each category, and for pooled cancers with good prognoses (luminal A + ILC) and for pooled cancers with poor prognoses (luminal B + HER 2 + TN).

Imaging data

Acquisition parameters are listed in Supplementary Table 1. All breast MRIs were performed on a single clinical 1.5-Tesla (T) scanner (MAGNETOM Aera, Siemens Healthcare) with the patient in the prone position with a dedicated 18-channel phased-array breast coil for signal reception. The MRI protocol before contrast injection included the following sequences: axial T2TSE, first phase of gradient-echoT1 VIBE with SPAIR (spectral attenuated inversion recovery) fat suppression (used as a mask for T1 VIBE subtraction), first phase of ultrafast TWIST-VIBE with Dixon fat suppression (Fig. 1). The injected contrast agent was gadoterate dimeglumine (Dotarem, Guerbet) intravenously infused in an antebrachial vein with a power injector (Spectris Solaris EP, MEDRAD) at a dose of 0.1 mmol/kg and at a rate of 2 ml/s, followed by a 20-ml saline flush. The ultrafast TWIST-VIBE sequence consisted of 9 phases with a first coding phase of 20.85 s followed by 8 phases with a temporal resolution of 7.1 s. The total acquisition time was 78 s. The TWIST technique allows high acceleration of 3D dynamic acquisition using a view-sharing technique and by alternating the acquisition of two k-space regions: a central k-space region "A" (related to overall image contrast) and a peripheral k-space region "B" (related image details). In this study, the TWIST k-space view-sharing parameters were 15% for region A and 25% for region B. Injection started at the end of the first coding phase. The VIBE sequence consisted of a pre-injection phase (mask) and 5 post-injection phases starting after the TWIST sequence, each lasting 1 min 20 s (Fig. 1). Subtraction and sagittal reconstruction were performed.

Image analysis

The examinations were interpreted on a SYNGO.VIA VAB11 image processing workstation (Siemens Healthcare).

Table 1 Demographic, clinical, and histological characteristics of the patients with malignant lesions

Characteristics	Malignant (n = 150)
Age (years), median (IQR)	51.0 (43–65)
BMI (kg/m^2) , median (IQR)	25.1 (22.0–29.7)
Hormonal status, n (%)	
Postmenopausal	65/150 (43.3%)
Premenopausal	85/150 (56.7%)
Familial history, n (%)	
No	115/150 (76.7%)
Yes	35/150 (23.3%)
Genetic risk, n (%)	
Standard	112/150 (74.7%)
Moderate	17/150 (11.3%)
High	21/150 (14%)
Histologic type, n/total n (%)	
Luminal A	30/150 (20%)
Luminal B	30/150 (20%)
HER2	30/150 (20%)
TN	30/150 (20%)
ILC	30/150 (20%)
Ki67, median (IQR)	0.3 (0.1–0.5)
ER, n/total n (%)	
+	108/150 (72.0%)
−	42/150 (28.0%)
PR, n/total n (%)	
+	85/150 (56.7%)
−	65/150 (43.3%)
SBR grade, n/total n (%)	
I	21/150 (14%)
II	85/150 (56.7%)
III	44/150 (29.3%)
Tumor size (mm), median (IQR)	25 (15–45)
LNI, n/total n (%)	
N +	77/150 (51.3)
N−	73/150 (48.7)
LVI[a], n/total n (%)	
No	69/89 (77.5%)
Yes	20/89 (22.5%)

Abbreviations. *BMI*, body mass index; *LNI*, lymph node invasion; *LVI*, lymphovascular involvement; *ER*, estrogen receptor; *PR*, progesterone receptor; *HER 2*, HER2 overexpression; *SBR*, Scarff–Bloom–Richardson; *TN*, triple negative; *ILC*, invasive lobular carcinoma; *IQR*, interquartile range

[a] In the 89 cases of surgery as the first therapeutic step

For each lesion selected, the enhancement curves from the TWIST-VIBE images and the VIBE images were obtained by using a 10-mm^2 minimum ROI manually positioned on the most intense color-coded maximum enhancement area. For TWIST-VIBE data, the measured parameter was the MS

Fig. 1 Breast MR protocol and enhancement curves from ultrafast TWIST-VIBE and conventional VIBE sequences. Abbreviations: T2, T2-weighted turbo spin-echo sequence; T1 VIBE+CM, 3DT1-weighted gradient-echo sequence with contrast medium injection; TWIST, ultrafast 3DT1 gradient

TWIST-VIBE parametric enhancement curve

VIBE semi-quantitative enhancement curve
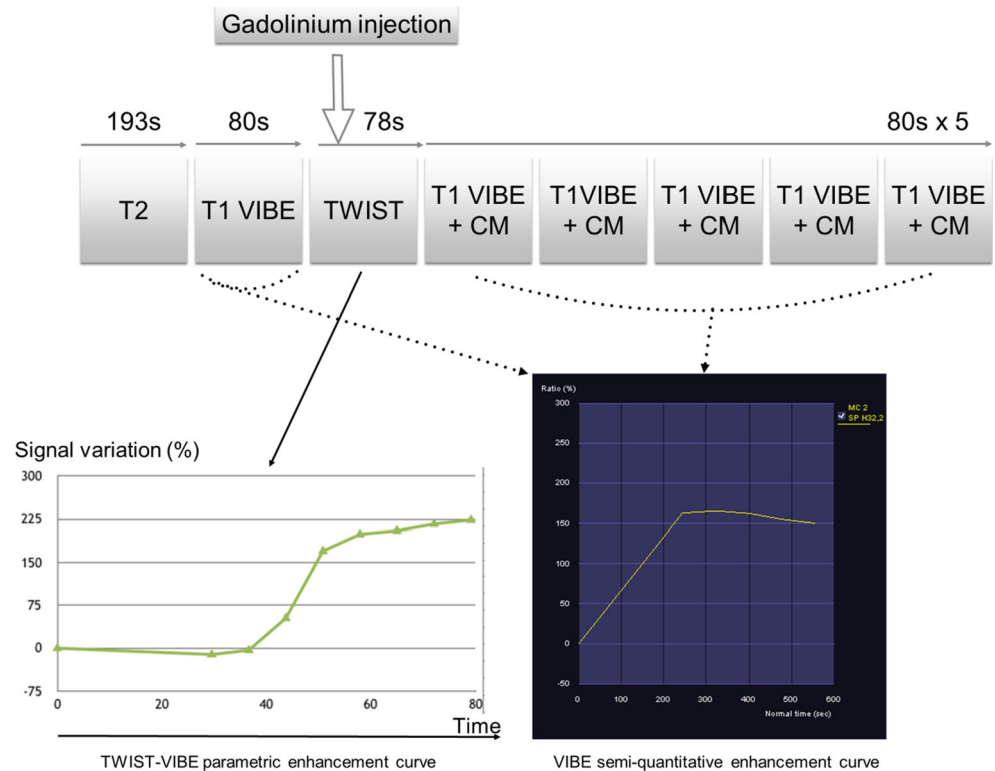
as defined by Mann et al in 2014 [14], based on the percentage variation in signal enhancement between two successive 7.1-s phases and expressed in percentage per second.

For the VIBE sequence, the semi-quantitative enhancement curves were performed as described by Kuhl et al and classified as 1 of 3 types [12]: type 1: progressive enhancement with signal increased by more than 10% between the early and late phase; type 2: intense enhancement with variation of the signal in absolute value < 10% between the early and late phase considered as a plateau; type 3: a decrease of more than 10% between the early and late phase. To compare semi-quantitative enhancement curves and measurement of the MS, we pooled type 2 and 3 curves in a category of suspicion of cancer, the type 1 curve being assimilated to a high probability of benignity.

Reproducibility study

Analysis of semi-quantitative curves obtained on VIBE sequences comprised one reading by a junior radiologist, and one reading by a senior radiologist with 22 years of experience.

Inter-observer agreement was assessed on the type of enhancement curve.

Statistical analysis

Quantitative parameters were described as median and interquartile range (IQR) due to a non-normal distribution, and qualitative parameters as frequency and percentage.

Inter-observer agreement was investigated with the Kappa value and its 95% confidence interval (95% CI). A value of > 0.6 was considered as strong agreement, and a value of > 0.8 as very strong agreement.

MS values of malignant and benign lesions were compared using a Mann–Whitney test. The discriminating power of the MS to predict malignant lesions was estimated with the AUC. The threshold was set according to the Youden Index to optimize both sensitivity and specificity. Results of the AUC, sensitivity, and specificity were expressed with 95% CIs. The same analysis was performed for the pooled luminal A + ILC group and for the pooled luminal B + HER 2 + TN group. The comparisons of sensitivities and specificities between MS and semi-quantitative curve analysis were performed by Mac Nemar test within the malignant lesions for sensitivities and within benign lesions for specificities.

The relationship between MS values and tumor characteristics was investigated with the Spearman correlation coefficient for quantitative parameters and with the Mann–Whitney test or Kruskal–Wallis test for qualitative parameters. All parameters with a p value less than 0.1 were introduced in a full multivariate linear regression. In the case of collinearity between two or more parameters, the most clinically relevant was chosen. In order to avoid overfitting, a simplification of this full model was performed by backward selection. The stability of the final model was investigated by the Bootstrap resampling method. The normality of the residuals was verified by a Q–Q normal plot. R^2 value was computed to

understand the proportion of variation in the MS explained by the included variables.

Agreement between the classification according to MS threshold values and that according to histological subcategories was quantified with weighted kappa and 95% CI. For analysis of discrepancies, quantitative parameters were compared using the Kruskal–Wallis test in the pooled luminal A + ILC group and with the Mann–Whitney test in the pooled luminal B + HER 2 + TN group. Qualitative parameters were compared with the chi-squared test or Fisher exact test. For luminal B + HER 2 + TN group, a multivariate analysis was performed. The log-linearity assumption of the logistic model was first checked. When this assumption was not verified, the quantitative parameter was transformed into binary variable according to clinical relevance or the median value. All parameters with a p value less than 0.1 in bivariate analyses were introduced in a full multivariate logistic regression model. In the case of collinearity between two or more parameters, the most clinically relevant was chosen. In order to avoid overfitting, a simplification of this full model was performed by backward selection. The stability of the final model was investigated by Bootstrap resampling method. The discriminative performance of the final model was assessed by the AUC and was considered as good when AUC > 0.8. Results were expressed as odds ratio and 95% confidence interval.

For all bivariate analyses, in case of significant results on the comparison of MS between more than 2 characteristics, MS values were compared two-to-two by post hoc tests with Bonferroni correction.

Statistical analyses were performed using SAS software, version 9.4 (SAS Institute Inc.). $p < 0.05$ was considered statistically significant.
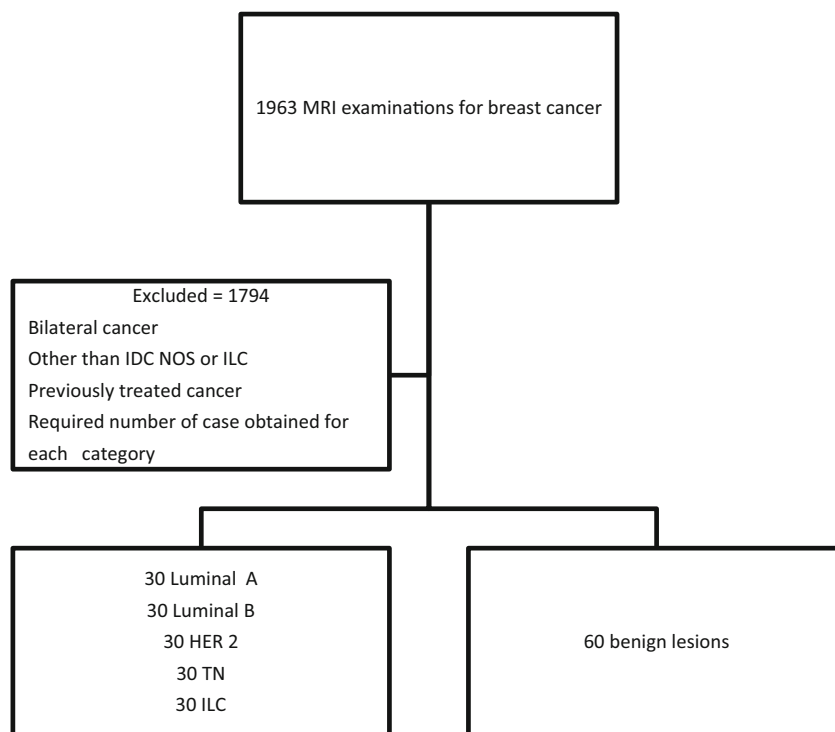
Results

Patient cohort

The 150 malignant lesions and the 60 benign lesions were observed in 169 patients with a median age of 49 years (IQR, 43–64). Flowchart is reported in Fig. 2.

Characteristics of the patients with malignant lesions are reported in Table 1.

Distinguishing benign from malignant lesions

The MS was significantly higher in malignant than in benign lesions (median 11.6, IQR (8.7–14.1) vs 3.6, IQR (2.7–4.7), $p < 0.001$). The area under the ROC curve was 0.94 (95% CI 0.91; 0.97) (Supplementary Figure 1). With a threshold of 6.5%/s, the sensitivity was 84% (95% CI 78%; 90%), and the specificity 90% (95% CI 82%; 97%).

Fig. 2 Flow chart. Abbreviations: IDC NOS, invasive ductal carcinoma non-otherwise specified; HER2, HER2 overexpression; TN, triple negative; ILC, invasive lobular carcinoma

| 1963 MRI examinations for breast cancer |

| Excluded = 1794 |
| Bilateral cancer |
| Other than IDC NOS or ILC |
| Previously treated cancer |
| Required number of case obtained for each category |

| 30 Luminal A |
| 30 Luminal B |
| 30 HER 2 |
| 30 TN |
| 30 ILC |

| 60 benign lesions |

Semi-quantitative curve analysis showed a sensitivity of 89% (95% CI 84%; 94%) and a specificity of 55% (95% CI 42%; 68%). Inter-observer agreement was very strong with a kappa of 0.81 (95% CI 0.75; 0.88). There was a significant difference between MS and semi-quantitative curve analysis for specificity ($p < 0.001$) but not for sensitivity ($p = 0.117$).

MS and clinical parameters, family history, genetic risk, and prognostic factors of breast cancer

Out of the 150 malignant lesions, the slope of enhancement in percentage per second was inversely correlated with age ($p < 0.001$) and BMI ($p = 0.025$), and was lower in postmenopausal women ($p < 0.001$) (Table 2). There was no correlation between the MS and family history ($p = 0.124$) or genetic risk ($p = 0.181$). The MS increased with tumor size ($p < 0.001$), value of the ki67-index ($p < 0.001$), absence of ER ($p < 0.001$), absence of PR ($p < 0.001$), SBR grading ($p < 0.001$), presence of LVI ($p < 0.001$), and presence of lymph node metastases ($p < 0.001$) (Table 2). In final multivariate analysis (Table 3), four independent parameters significantly explained MS value ($R^2 = 0.32$): MS values decreased with BMI increasing ($p = 0.035$), postmenopausal status ($p < 0.001$) and positive ER status ($p < 0.001$) and increased with tumor size ($p < 0.001$).

MS and histological subcategories

MS was significantly different according to histological type ($p < 0.001$, Table 3). Luminal A had a significantly lower MS than TN ($p = 0.04$) and ILC had lower MS values than luminal B ($p = 0.03$), HER2 ($p < 0.01$), and TN ($p < 0.01$) (Supplementary Figure 2). MS was significantly lower for the pooled luminal A + ILC group than for the pooled luminal B + HER2 + TN group featuring tumors with poorer prognoses (8.9, IQR (5.5–12.1) compared to 12.9, IQR (10.6–15.7), $p < 0.001$). The AUC was 0.76 (95% CI 0.68; 0.84) (Supplementary Figure 3). With a threshold of 11%/s, the sensitivity to identify invasive carcinoma subtypes with poorer prognoses was 71% (95% CI 62%; 80%), and the specificity 68% (95% CI 57%; 80%).

The first cut-off of 6.5%/s to distinguish benign from malignant lesions and the second cut-off of 11%/s to distinguish good from poor prognosis groups showed strong agreement with histologic categories, with a weighted Kappa at 0.61 (95% CI 0.53; 0.69) (Supplementary Material eTable2).

Analysis of discrepancies between classification of lesions according to MS values and histological subcategories

Table 4 details all lesion characteristics according to MS classification. In the luminal A + ILC group, lesions with MS < 6.5%/s

Table 2 Relationship between patient characteristics, prognostic factors, and maximum slope of enhancement in percentage per second in the patients with malignant lesions

	MS in percentage per second	p value
Age, ρ [95% CI]	ρ = -0.37 [−0.51; −0.23]	< 0.001
BMI, ρ [95% CI]	ρ = −0.18 [−0.33; −0.02]	0.025
Hormonal status, median (IQR)		< 0.001
Postmenopausal	10.0 (6.2–12.7)	
Premenopausal	12.5 (10.2–15.7)	
Familial cancer, median (IQR)		0.124
Yes	11.9 (9.5–14.1)	
No	10.3 (8.2–13.6)	
Genetic risk, median (IQR)		0.181
Standard	11.0 (7.6–13.8)	
Moderate	11.9 (11.2–14.1)	
High	12.3 (10.3–15.5)	
Histological type, median (IQR)		< 0.001
Luminal A	9.5 (5.5–13.2)	
Luminal B	11.6 (9.5–13.8)	
HER 2	13.1 (10.9–18)	
TN	13.3 (11.6–15.7)	
ILC	8.4 (5.7–10.8)	
Ki67, ρ [95% CI]	ρ = 0.29 [0.14; 0.44]	< 0.001
ER, median (IQR)		< 0.001
+	10.5 (7–13.2)	
−	13.3 (11.6–18)	
PR, median (IQR)		< 0.001
+	10.6 (7.2–13.1)	
−	13.2 (10.4–16.4)	
SBR grade, median (IQR)		< 0.001
I	8.2 (5.4–10.2)	
II	11.5 (7.3–14)	
III	13.2 (11.1–16.1)	
LNI, median (IQR)		< 0.001
N+	12.6 (10.7−16)	
N−	10.2 (6.4–13.2)	
LVI[Δ], median (IQR)		< 0.001
No	9.5 (5.6–11.5)	
Yes	13.1 (10.7–14.8)	
Tumor size, ρ [95% CI]	ρ = 0.33 [0.18; 0.46]	< 0.001

[Δ] In the 89 cases of surgery as the first therapeutic step

Abbreviations: *MS*, maximum slope; *BMI*, body mass index; *HER2*, HER2 overexpression; *TN*, triple negative; *ILC*, invasive lobular carcinoma; *ER*, estrogen receptor; *PR*, progesterone receptor; *SBR*, Scarff–Bloom–Richardson; *LNI*, lymph node involvement; *LVI*, lymphovascular involvement; *IQR*, interquartile range; *ρ*, Spearman correlation coefficient; *CI*, confidence interval

were significantly smaller ($p < 0.001$). After Bonferroni correction, Tsize was significantly lower for lesions with MS < 6.5%/s comparatively to lesions with MS from 6.5%/s to < 11%/s ($p =$

Table 3 Linear multivariate models for explaining maximum slope of enhancement in percentage per second in the patients with malignant lesions

	Full multivariate model$^{\Delta}$		Final multivariate model‡	
	Parameter estimate (standard error)	p value	Parameter estimate (standard error)	p value
Intercept	15.77 (2.19)	< 0.001	17.38 (1.97)	< 0.001
BMI (kg/m^2)	−0.15 (0.07)	0.032	−0.15(0.07)	0.035
Hormonal status				
Premenopausal	0	-	0	
Postmenopausal	−2.63 (0.7)	< 0.001	−2.72(0.69)	< 0.001
Ki67	−0.61 (2.06)	0.769	-	
ER				
+	−2.10 (1.18)	0.078	−3.18(0.76)	< 0.001
−	0	-	0	
PR				
+	−0.99 (0.97)	0.312	-	
−	0	-		
SBR grade				
I	0	-		
II	1.64 (1.11)	0.14	-	
III	1.8 (1.42)	0.207		
LNI				
N+	1.29 (0.76)	0.089	-	
N−	0	-		
Tumor size (mm)	0.04 (0.02)	0.013	0.06 (0.01)	< 0.001

$^{\Delta}$ Age not included since strongly correlated with hormonal status; histological type not included since strongly correlated with ki67, ER, and PR; lymphovascular involvement not included since only available if surgery as the first therapeutic step

‡ After backward selection and validation of its stability with the Bootstrap resampling method

Abbreviations: *BMI*, body mass index; *ER*, estrogen receptor; *PR*, progesterone receptor; *SBR*, Scarff–Bloom–Richardson; *LNI*, lymph node involvement

0.005) and lesions with MS ≥ 11%/s ($p = 0.003$) but not between lesions with MS from 6.5%/s to < 11%/s and lesions with MS ≥ 11%/s ($p = 1$). In the luminal B + HER2 + TN group, a significantly higher number of lesions with a MS of between 6.5%/s and 11%/s was observed in older and postmenopausal women ($p = 0.009$ and $p = 0.005$, respectively), and in lesions with smaller size ($p = 0.006$), lower ki67-index values ($p = 0.046$), less frequent ER and PR negative status ($p = 0.003$ and $p = 0.001$), and no LVI or LNI ($p = 0.024$ and $p = 0.013$). MS classification was also different according to histological type ($p = 0.016$) with a significant difference between luminal B and TN after Bonferroni correction ($p = 0.014$). In final multivariate analysis, three independent parameters explained a MS < 11%/s: postmenopausal status ($p = 0.005$), a tumor size less than 20 mm ($p = 0.014$) and positive ER status ($p = 0.002$) (Table 5). The discriminative performance of the final model was considered as good (AUC = 0.82, 95% CI 0.73; 0.91). In this group, two lesions had MS < 6.5%/s and were both luminal B tumors of 1.1 and 1.2 cm without LVI or LNI (Supplementary Material e Table 3).

Discussion

Our study reports that MS cut-off at 6.5%/s could discriminate benign from malignant lesions, with sensitivity and specificity of 84% and 90%, respectively. The MS was inversely correlated with age and BMI, and was lower in postmenopausal women and increased with tumor size, ki67-index value, absence of estrogen receptor (ER) and progesterone receptor (PR), SBR grading, presence of lymphovascular involvement, and lymph node invasion. The MS appears to be significantly higher in tumors of luminal B, HER2 and TN subtypes, which are associated with poorer prognoses, than in tumors of the luminal A and ILC subtypes. With a threshold of 11%/s, the sensitivity and specificity to identify invasive carcinoma subtypes with poorer prognoses were 71% and 68%, respectively. Considering these results, a first MS threshold of 6.5%/s may indicate malignancy and a second of 11%/s may show a tumor with poor prognosis.

The correlation between the MS value expressed and malignancy of breast lesions was reported by some previous

Table 4 Analysis of the discrepancies between the classification of lesions according to the MS and to histological subcategories of breast cancer

	Luminal A + ILC			
	Underestimated	Correctly estimated	Overestimated	p value
	MS < 6.5%/s	6.5%/s ≤ MS < 11%/s	MS ≥ 11%/s	
Age (years), median (IQR)	65.5 (56–69)	57 (49–67)	54 (42–67)	0.105
BMI, median (IQR)	24.5 (23–28.7)	26.9 (22.9–31.7)	22 (19.6–30)	0.064
Familial cancer, n (%)	6/22 (27.3%)	6/19 (31.6%)	1/19 (5.3%)	0.096
Genetic risk, n (%)				0.632
Standard	20/22 (90.9%)	15/19 (78.9%)	17/19 (89.5%)	
Moderate	1/22 (4.55%)	4/19 (21.1%)	2/19 (10.5%)	
High	1/22 (4.55%)	0/19 (0%)	0/19 (0%)	
Postmenopausal, n (%)	17/22 (77.3%)	10/19 (52.6%)	9/19 (47.4%)	0.109
Ki67, median (IQR)	0.1 (0.1–0.1)	0.1 (0.1–0.1)	0.1 (0.1–0.2)	0.331
T size (mm), median (IQR)	12 (9–16)	26 (16–41)	25 (19–45)	< 0.001
LVI, n (%)	1/21 (4.8%)	3/17 (17.6%)	4/16 (25.0%)	0.205
LNI, n (%)	4/22 (18.2%)	9/19 (47.5%)	8/19 (42.1%)	0.109
PR negative, n (%)	7/22 (31.8%)	3/19 (15.8%)	2/19 (10.5%)	0.239
ER negative, n (%)	0/22 (0%)	0/19 (0%)	0/19 (0%)	-
SBR grade, n (%)				0.375
I	9/22 (40.9%)	7/19 (36.8%)	4/19 (21.1%)	
II	13/22 (59.1%)	11/19 (57.9%)	15/19 (78.9%)	
III	0/22 (0%)	1/19 (5.3%)	0/19 (0%)	
Histological type, n (%)				0.268
Luminal A	11/22 (50.0%)	7/19 (36.8%)	12/19 (63.2%)	
ILC	11/22 (50.0%)	12/19 (63.2%)	7/19 (36.8%)	

	Luminal B + HER 2 + TN		
	Underestimated	Correctly estimated	p value
	MS < 11%/s	MS ≥ 11%/s	
Age (years), median (IQR)	55 (45–67)	45.5 (38.5–53)	0.009
BMI, median (IQR)	27.4 (24.1–31.3)	24.7 (22–28.5)	0.060
Familial cancer, n (%)	9/26 (34.6%)	13/64 (20.3%)	0.152
Genetic risk, n (%)			0.238
Standard	21/26 (80.8%)	39/64 (60.9%)	
Moderate	3/26 (11.5%)	13/64 (20.3%)	
High	2/26 (7.7%)	12/64 (18.8%)	
Postmenopausal, n (%)	14/26 (53.9%)	15/64 (23.4%)	0.005
Ki 67, median (IQR)	0.4 (0.3–0.5)	0.4 (0.3–0.6)	0.046
T size (mm), median (IQR)	20 (16–34)	34 (22–54)	0.006
LVI, n (%)	3/18 (16.7%)	9/17 (52.9%)	0.024
LNI, n (%)	11/26 (42.3%)	45/64 (70.3%)	0.013
PR negative (%)	9/26 (34.6%)	44/64 (68.7%)	0.003
ER negative, n (%)	5/26 (19.2%)	37/64 (57.8%)	0.001
SBR grade, n (%)			0.146
I	1/26 (3.8%)	0/64 (0%)	
II	15/26 (57.7%)	31/64 (48.4%)	
III	9/26 (34.5%)	33/64 (51.6%)	
Histological type, n (%)			0.016
Luminal B	14/26 (53.8%)	16/64 (25.0%)	
HER 2	8/26 (30.8%)	22/64 (34.4%)	
TN	4/26 (15.4%)	26/64 (40.6%)	

Abbreviations: *MS*, maximum slope; *BMI*, body mass index; *T*, tumor; *LNI*, lymph node involvement; *LVI*, lymphovascular involvement; *ER*, estrogen receptor; *PR*, progesteron receptor; *SBR*, Scarff–Bloom–Richardson; *HER2*, HER2 overexpression; *TN*, triple negative; *ILC*, Invasive lobular carcinoma; *IQR*, interquartile range

Table 5 Bivariate and multivariate analyses to assessed parameters explaining the underestimation of the classification according to the MS (MS < 11%/s) to classify luminal B + HER2 + TN subcategories of breast cancer

	Bivariate analyses		Full multivariate model		Final multivariate model[‡]	
	OR and 95% CI	p value	OR and 95% CI	p value	OR and 95% CI	p value
Age (years)[1]						
< 60	1		1			
≥ 60	3.38 [1.19; 9.54]	0.022	1.22 [0.15; 9.99]	0.856	-	
BMI (kg/m²)[1]						
< 25	1		1			
≥ 25	3.08 [1.14; 8.33]	0.027	3.38 [0.99; 11.6]	0.052	-	
Hormonal status						
Premenopausal	1		1		1	
Postmenopausal	3.81 [1.45; 9.99]	0.006	4.38 [0.62; 30.84]	0.138	5.27 [1.65; 16.96]	0.005
Ki 67[2]						
≤ 0.4	2.89 [1.07; 7.81]	0.037	1.05 [0.28; 4.01]	0.938	-	
> 0.4	1		1			
T size[2] (mm)						
≤ 20	4.59 [1.71; 12.2]	0.002	3.6 [1.03; 12.55]	0.045	4.01 [1.33; 12.08]	0.014
> 20	1		1		1	
LNI						
N+	1		1			
N−	3.23 [1.26; 8.31]	0.015	2.99 [0.9; 9.99]	0.075	-	
PR						
+	4.16 [1.58; 10.91]	0.004	0.73 [0.13; 4.01]	0.713	-	
-	1		1			
ER						
+	5.75 [1.93; 17.19]	0.002	9.51 [1.24; 72.7]	0.030	7.29 [2.05; 25.96]	0.002
−	1		1		1	
Histological type[3]						
Luminal B	5.69 [1.59; 20.33]	0.009				
HER 2	2.36 [0.63; 8.92]	0.986				
TN	1					

[1] Dichotomized according to clinical relevance

[2] Dichotomized according to median value in the luminal B + HER 2 + TN group

[3] Not included in the full multivariate model since strongly correlated to ki67, ER, and PR

[‡] After backward selection and validation of its stability with Bootstrap resampling method

Abbreviations: *BMI*, body mass index; *T*, tumor; *LNI*, lymph node involvement; *ER*, estrogen receptor; *PR*, progesteron receptor; *HER2*, HER2 overexpression; *TN*, triple negative; *ILC*, invasive lobular carcinoma; *OR*, odds ratio; *95% CI*, 95% confidence interval

studies [14, 15, 17–21] and the cut-off of 6.5%/s (here, on a 1.5-T scanner) was similar to findings reported by Mann et al (6.4%/s) and by Goto et al (7.3%/s) (both on a 3-T scanner) [14, 15]. The sensitivity of 90% and a specificity of 67% were reported in the study by Mann [14]. Ohashi et al reported a discriminant MS threshold of 9.76%/s with a k-space weighted image contrast (KWIC) sequence achieving a sensitivity of 91.1% and a specificity of 62.5% [18]. However, further investigation is required, as some studies have reported

contrasting results. Shin et al did not observe any correlation between the MS and the probability of malignancy using a TWIST-VIBE sequence at 3 T [19], and their reported MS value was much higher (mean of 127.9%/s in malignancies) than those reported here and by Mann. Honda et al reported a MS cut-off of 20.1%/s to distinguish malignant from benign lesions [17]. MS values could vary depending on parameters such as the type of sequence used, or the relaxivity of the contrast agent.

Using ultrafast sequences and measuring the MS increases the specificity of breast DCE-MRI compared to analysis of semi-quantitative curves alone. The limitations of semi-quantitative analysis of enhancement kinetics in curves are known from their initial description by Kuhl et al in 1999 [12]. It was reported that 17% of benign lesions presented enhancement of type 2 and 3 curves, and 8.9% of cancers exhibited enhancement of type 1 [12]. In addition, analysis of enhancement kinetics by using semi-quantitative curves requires a longer acquisition time taking 7 to 8 min, which lengthens the MRI examination time. Semi-quantitative curves could therefore be replaced by measurement of the MS obtained with ultrafast sequences, as previously reported [14, 17, 18, 20]. If so, it would not be necessary to perform delayed MRI scans for 7 or 8 min, and examination times could be shortened.

The relationship between high BMI and lower MS may indicate hormonal-dependent luminal cancer more often associated with obesity and postmenopause [22–24]. The increase in the relative risk of developing breast cancer was reported to be 1.1 per 5 BMI units, especially for ER-positive IDC [22]. Lyengar et al reported a 56% increase in the risk of developing ER-positive breast cancer per 5-kg increase of trunk fat, despite a normal BMI [24].

The correlations between MS and tumor size and histo-prognostic parameters reported in our study were consistent with the findings of Goto et al [15]. However, these findings disagree with those of Shin et al, who found no significant correlation between MS and histo-prognostical parameters [19]. Some of our results appear original. Based on the 2 multivariate analyses, we reported that menopausal status, tumor size, and ER status were independent factors explaining MS value, not only in patients with malignant lesions, but also in the sub-groups of patients with poorer prognosis. To our knowledge, these robust and consistent results for these 3 parameters were not reported before.

Our study has certain limitations. First, it is a monocentric work on a single machine. A study of MS measurements on different machines and at different magnetic field strengths to determine the generalizability of our findings has not yet been performed. A comparison of the measurement of the MS, and the morphological analysis according to the BI-RADS lexicon, and a complete protocol combining morphological sequences and dynamic sequences, was not carried out in our study. The diagnostic accuracy of MS alone in Ohashi's study was inferior to morphological analysis. However, it has been reported that the diagnostic accuracy of the morphological analysis according to BI-RADS can be improved by the addition of the MS measurement [15, 20, 25]. Finally, we did not analyze lesion enhancement time compared to the aorta or internal mammary vessels described in the literature as improving the specificity of MRI [15, 17, 19, 20, 25, 26]. Our ultrafast TWIST sequence had repeated phases every 7 s. Mus et al showed that lesions whose enhancement began less than 10 s after aortic enhancement were more specifically malignant and lesions whose enhancement began more than 15 s after aortic enhancement were benign. However, the ultrafast sequence used included repeated phases of 4.3 s in their work [26]. The insufficient temporal resolution of the sequence used in our study did not allow us to show significant enhancement time differences between the lesions.

Conclusion

The MS obtained with ultrafast breast DCE- MRI is an emerging tool in the characterization of breast lesions. Our study at 1.5 T indicates that measurement of the MS not only distinguishes benign from malignant lesions but also can distinguish between lesions with good and poor prognoses. The generalizability of the findings needs further investigation in a larger study.

Declarations

Guarantor The scientific guarantor of this publication is Philippe Henrot.

Statistics and biometry One of the authors has significant statistical expertise.

Informed consent Written informed consent was waived by the institutional review board.

Ethical approval Institutional review board approval was obtained.

Conflict of interest Khalid Ambarki is a Siemens Healthcare GmbH employee.
 Other authors have no potential conflict of interest to declare.

Methodology
• retrospective
• observational
• performed at one institution

References

1. Peters NH, Borel Rinkes IH, Zuithoff NP et al (2008) Meta-analysis of MR imaging in the diagnosis of breast lesions. Radiology 246: 116–124

2. Medeiros LR, Duarte CS, Rosa DD et al (2011) Accuracy of magnetic resonance in suspicious breast lesions: a systematic quantitative review and meta-analysis. Breast Cancer Res Treat 126:273–285

3. Bennani-Baiti B, Baltzer PA (2017) MR imaging for diagnosis of malignancy in mammographic microcalcifications: a systematic review and meta-analysis. Radiology 283:692–701

4. Morris EA, Comstock CE, Lee CH et al (2013) ACR BI-RADS® magnetic resonance imaging. In: ACR BI-RADS® Atlas, Breast Imaging Reporting and Data System. American College of Radiology, Reston

5. Pinker-Domenig K, Bogner W, Gruber S et al (2012) High resolution MRI of the breast at 3 T: which BI-RADS(R) descriptors are most strongly associated with the diagnosis of breast cancer? Eur Radiol 22:322–330

6. Mann RM, Kuhl CK, Kinkel K, Boetes C (2008) Breast MRI: guidelines from the European Society of Breast Imaging. Eur Radiol 18:1307–1318

7. Sardanelli F, Boetes C, Borisch B et al (2010) Magnetic resonance imaging of the breast: recommendations from the EUSOMA working group. Eur J Cancer 46:1296–1316

8. Boetes C, Barentsz JO, Mus RD et al (1994) MR characterization of suspicious breast lesions with a gadolinium-enhanced Turbo-FLASH subtraction technique. Radiology 193:777–781

9. Heywang SH, Wolf A, Pruss E, Eiermann W, Permanetter W (1989) MR imaging of the breast with Gd-DTPA: use and limitations. Radiology 171:95–103

10. Kaiser WA, Zeitler E (1989) MR imaging of the breast: fast imaging sequences with and without Gd-DTPA—preliminary observations. Radiology 170:681–686

11. Fischer U, von Heyden D, Vosshenrich R, Vieweg I, Grabbe E (1993) Signalverhalten maligner und benigner la¨sionen in der dynamischen 2D-MRT der mamma. Rofo 158:287–292

12. Kuhl CK, Mielcareck P, Klaschik S et al (1999) Dynamic breast MR imaging: are signal intensity time course data useful for differential diagnosis of enhancing lesions? Radiology 211:101–110

13. Le Y, Kipfer H, Majidi S et al (2013) Application of time-resolved angiography with stochastic trajectories (TWIST)-Dixon in dynamic contrast-enhanced (DCE) breast MRI. J Magn Reson Imaging 38:1033–1042

14. Mann RM, Mus RD, van Zelst J, Karssemeijer N, Platel B (2014) A novel approach to contrast-enhanced breast magnetic resonance imaging for screening: high-resolution ultrafast dynamic imaging. Invest Radiol 49:579–585

15. Goto M, Sakai K, Yokota H et al (2018) Diagnostic performance of initial enhancement analysis using ultra-fast dynamic contrast-enhanced MRI for breast lesions. Eur Radiol 29:1164–1174

16. Herrmann KH, Baltzer PA, Dietzel M et al (2011) Resolving arterial phase and temporal enhancement characteristics in DCE MRM at high spatial resolution with TWIST acquisition. JMRI 34:973–982

17. Honda M, Kataoka M, Onishi N et al (2020) New parameters of ultrafast dynamic contrast-enhanced breast MRI using compressed sensing. JMRI 51:164–174

18. Ohashi A, Kataoka M, Kanao S et al (2019) Diagnostic performance of maximum slope: a kinetic parameter obtained from ultrafast dynamic contrast-enhanced magnetic resonance imaging of the breast using k-space weighted image contrast (KWIC). Eur J Radiol 118:285–292

19. Shin SU, Cho N, Kim SY, Chang JM, Moon WK (2020) Time-to-enhancement at ultrafast breast DCE-MRI: potential imaging biomarker of tumour aggressiveness. Eur Radiol 30:4058–4068

20. Milon A, Vande Perre S, Poujol J et al (2019) Abbreviated breast MRI combining FAST protocol and high temporal resolution (HTR) dynamic contrast enhanced (DCE) sequence. Eur J Radiol 117:199–208

21. Lee SJ, Ko KH, Jung HK, Koh JE, Park AY (2020) The additional utility of ultrafast MRI on conventional DCE-MRI in evaluating preoperative MRI of breast cancer patients. Eur J Radiol 124:1–9

22. Lauby-Secretan B, Scoccianti C, Loomis D et al (2016) International Agency for Research on Cancer Handbook Working Group. Body fatness and cancer: viewpoint of the IARC Working Group. N Engl J Med 375:794–798

23. Trentham-Dietz A, Newcomb PA, Storer BE et al (1997) Body size and risk of breast cancer. Am J Epidemiol 145:1011–1019

24. Lyengar NM, Arthur R, Manson JE et al (2019) Association of body fat and risk of breast cancer in postmenopausal women with normal body mass index: a secondary analysis of a randomized clinical trial and observational study. JAMA Oncol 5:155–163

25. Platel B, Mus RD, Welte T, Karssemeijer N, Mann R (2014) Automated characterization of breast lesions imaged with an ultrafast DCE-MR protocol. IEEE Trans Med Imaging 33:225–232

26. Mus RD, Borelli C, Bult P et al (2017) Time to enhancement derived from ultrafast breast MRI as a novel parameter to discriminate benign from malignant breast lesions. Eur J Radiol 89:90–96